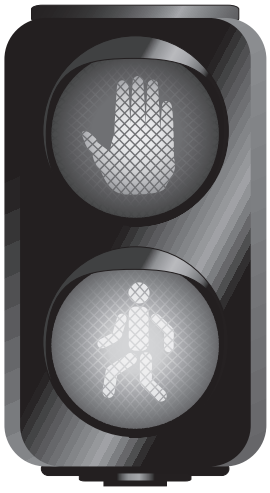

Six

Failure of Stop and Go in *de novo* Parkinson's disease - a functional magnetic resonance imaging study

Chris Vriend
Niels J.H.M. Gerrits
Henk W. Berendse
Dick J. Veltman
Odile A. van den Heuvel
Ysbrand D. van der Werf

Neurobiology of Aging 2015; 36:470-75

Abstract

Behavioral impairments in response inhibition and initiation are common in Parkinson's disease (PD) and are associated with reduced impulse control. No prior study, however, has investigated the functional correlates of response inhibition in de novo PD. Twenty-one de novo PD patients and 37 matched healthy controls performed a stop-signal task during fMRI. The results showed that PD patients, compared with healthy controls, were slower on response initiation but not inhibition. Task-related activation of the response inhibition network, including the inferior frontal gyrus, was reduced in PD patients and the activity in the inferior frontal gyrus correlated negatively with motor symptom severity. These findings show that de novo PD patients exhibit functional deficits in the response inhibition network which are partly related to disease pathology and already evident prior to commencing dopamine replacement therapy. This study provides insights into the neural underpinnings of impulse control deficits, relevant for the study of the neural vulnerability factors involved in the development of impulse control disorders in PD.

Introduction

Parkinson's disease is a progressive neurodegenerative disorder that affects, among others, dopaminergic afferents towards the striatum (Kish *et al.* 1988; Braak *et al.* 2004). This striatal dopaminergic denervation lies at the root of the Parkinson-related motor disturbances but there is growing evidence that it is also involved in the development of non-motor symptoms, such as depression (Hesse *et al.* 2009; Vriend *et al.* 2014d), and impulse control disorders (ICD) (Voon *et al.* 2014; Vriend *et al.* 2014b). ICD are characterized by an inability to suppress certain (potentially dangerous) impulses (American Psychiatric Association 2013). It is hypothesized that ICD in Parkinson's disease arise after commencing dopamine replacement therapy in patients with a certain neurobiological susceptibility (Vriend *et al.* 2014c). Nevertheless, non-clinically significant deficits in impulse control have also been described in Parkinson patients without ICD (Aarts *et al.* 2012; van der Vegt *et al.* 2013; Ye *et al.* 2014b). Response inhibition is a frequently used measure of the ability to control one's impulses in an experimental setting (Aron 2011). Response inhibition tasks require subjects to inhibit inappropriate responses when certain cues are provided. Previous behavioral studies have shown deficits in response inhibition in patients with Parkinson's disease compared with healthy controls (Gauggel *et al.* 2004; Obeso *et al.* 2011a; Nombela *et al.* 2014). Furthermore, these deficits in response inhibition in Parkinson's disease correlated with alterations in neurophysiological markers (Bokura *et al.* 2005; Beste *et al.* 2009; Beste *et al.* 2010), and were associated with altered brain activity patterns (Farid *et al.* 2009; Baglio *et al.* 2011) and reductions in frontal-striatal brain volume (O'Callaghan *et al.* 2013b). However, all previous studies were carried out in Parkinson patients that were on dopamine replacement therapy, making it impossible to disambiguate the consequences of (chronic) medication from the pathophysiological alterations associated with the disease itself. Nevertheless, two previous studies employing an ON/OFF paradigm showed that levodopa is unable to fully restore deficits in response inhibition (Farid *et al.* 2009; Obeso *et al.* 2011b), suggesting that the deficits are primarily due to pathophysiological changes.

The stop-signal task exerts higher demands on subjects compared with the Go/No-Go task that was employed in almost all previous neuroimaging studies in Parkinson's disease (Sebastian *et al.* 2013a). Therefore, the stop-signal task puts higher strain on the compensational resources of the inhibition network and is thus more likely to reveal subtle between-group differences in brain activation. This was also observed in a very recent paper that showed decreased activation of the right inferior frontal gyrus in medicated Parkinson's disease patients compared with healthy controls during performance of a stop-signal task (Ye *et al.* 2014b). Based on this and other previous studies, we hypothesized that, compared with healthy controls, de novo Parkinson patients would show impairments in response initiation and inhibition concomitant with hypoactivation of inhibition-

related brain areas.

Methods

Participants

Parkinson patients were recently diagnosed by a movement disorder specialist according to the UK Parkinson's disease Brain Bank criteria (Daniel and Lees 1993) for idiopathic Parkinson's disease. All patients were naive for dopamine replacement therapy (de novo). We used the Unified Parkinson's Disease Rating Scale motor section (UPDRS-III) (Fahn *et al.* 1987) and Hoehn and Yahr stage (Hoehn and Yahr 1967) to assess disease severity and disease stage, respectively. Healthy controls were recruited through advertisements. Exclusion criteria in healthy controls were all current or previous severe traumatic head injuries, other neurological or psychiatric disorders, including alcohol or drug dependence. Exclusion criteria in Parkinson's disease were a current or previous psychiatric or neurological disorder other than Parkinson's disease itself. Participants were screened for the presence of psychiatric disorders using the Structured Clinical Interview for DSM-IV Axis-I Disorders (SCID-I) (First *et al.* 2002) and for signs of dementia using the Mini Mental State Examination (MMSE) (Folstein *et al.* 1975). All participants with excessive movement during functional MRI scanning (>3mm) or use of centrally active drugs were excluded. We administered the Dutch version of the national adult reading test (Schmand *et al.* 1991) to provide a measure of pre-morbid intelligence. All participants provided written informed consent according to the declaration of Helsinki and the study was approved by the local research ethics committee.

Stop-signal task

Participants performed a visual stop-signal task during fMRI scanning (de Wit *et al.* 2012) in which they responded to the direction of an arrow (left or right) by pressing a button with the index finger of the concordant hand (Go-trials). Go-trials were interspersed pseudo-randomly with Stop-trials, in which a cross was superimposed on the arrow with some delay after the initial presentation of the arrow. On these trials, participants had to refrain from responding. The delay of the stop-signal (stop-signal delay or SSD) was continuously adapted by a staircase tracking mechanism to approximate a 50% inhibition on all stop-trials. Participants were instructed to respond quickly but accurately. They were also told that the design of the task would prevent them from accurately inhibiting their responses on all Stop-trials. Further details on the task are provided in the supplementary methods. Behaviorally, we measured the mean reaction time on successful Go-trials (speed of Go process), the stop-signal reaction time (speed of Stop process) and the error percentage on Go-trials and Stop-trials. Participants with a Go-trial error percentage >40% were excluded; cf. (Congdon *et al.* 2012). Stop-

signal reaction time (SSRT) was estimated with to the integration method, which according to simulations gives to most reliable estimate of SSRT (Verbruggen *et al.* 2013). Because response latencies gradually increased during the task, SSRTs were estimated separately in four smaller blocks (each block consisting of at least 50 trials) and subsequently averaged. Blocks from subjects with stop-trial error percentages <25% or >75% were excluded (Congdon *et al.* 2012).

Image acquisition

Imaging data were collected using a GE Signa HDxT 3T MRI scanner (General Electric, Milwaukee, U.S.) at the VU University Medical Center (Amsterdam, The Netherlands). Task stimuli were projected on a screen behind the participant's head at the end of the scanner table, visible through a mirror mounted on the head coil. The participant's head was immobilized using foam pads to reduce motion artifacts.

T2*-weighted echo-planar images (EPI's) with blood oxygenation level-dependent (BOLD) contrast were acquired in each session; slice order: sequential and ascending, TR=2100 ms, TE=30 ms, flip angle=80°, 40 slices (3.75 x 3.75 mm in-plane resolution; 2.8 mm slice thickness; matrix size 64 x 64) per EPI volume. Structural images were acquired using a 3D sagittal T1-weighted sequence (TI=450 ms, TE=3 ms, voxel size 1 x 0.977 x 0.977 mm, 172 slices). In addition, we acquired [123I]FP-CIT ([123I]N-ω-Fluoropropyl-2β-carbomethoxy-3β-(4-iodophenyl) nortropane) SPECT scans from a subgroup of PD patients to measure presynaptic striatal dopamine transporter availability as a measure for striatal dopamine integrity. Dopamine transporter availability was measured in the ventral striatum, anterior-dorsal striatum and posterior putamen. See the supplementary material for a full description of the [123I]FP-CIT SPECT acquisition and delineation of the region's of interest.

Data preprocessing and analyses

Behavioral analyses were conducted in IBM SPSS 20 (Armonk, NY, USA). Between-group differences were analyzed with two-sample T-tests or Mann-Whitney U-tests, depending on the variable's distribution. Correlations between behavior and clinical measures were analyzed with Pearson's r correlation coefficient.

Imaging preprocessing and analyses were performed with SPM8 (Wellcome Trust Center for Neuroimaging, London, UK). Functional brain images were manually reoriented, slice-time corrected and realigned to the first volume. The resulting mean image was then co-registered to the structural T1 image, and images were normalized to Montreal Neurological Institute (MNI) space and spatially smoothed using an 8 mm Full-Width-at-Half-Maximum (FWHM) Gaussian kernel. All imaging analyses were performed in the context of the general linear model. Onsets of successful Go-trials, successful Stop-trials and unsuccessful Stop-trials were modeled per participant (first-level) using delta functions

convolved with the hemodynamic response function. Participants' movement parameters (3 translation and 3 rotation parameters) were added as additional regressors of no interest. A 128 s high-pass filter was used to remove noise associated with low-frequency confounds. Inhibition-related blood-oxygen-level dependent (BOLD) activity was modeled by contrasting successful Stop-trials with successful Go-trials (Successful Stop>Successful Go). Error-related activity was probed by contrasting unsuccessful Stop-trials with successful Stop-trials. These contrasts were brought into second-level random effects analyses.

We examined between-group differences using two-sample T-tests in a priori selected brain regions by constructing spherical functional regions of interest (ROI) (MarsBaR, http://marsbar.sourceforge.net) with a 10 mm radius around the peak voxel coordinates of the main effects of 73 healthy controls, pooled from the current study and one conducted previously (de Wit *et al.* 2012). Differences in inhibition-related activity (Successful Stop>Successful Go) were probed in the left and right inferior frontal gyrus (right: [x=51, y=20, z=7]; left: [x=-54, y=17, z=4]), inferior parietal lobule (right: [x=35, y=-64, z=46]; left: [x=-33, y=-64, z=37]), caudate nucleus (right: [x=12, y=11, z=4]; left: [x=-12, y=14, z=1]) and pre-supplementary motor area (right: [x=5, y=29, z=43]). Neither the left pre-supplementary motor area nor subthalamic nuclei showed peak voxel activity in the main effects of the pooled healthy control samples. We also examined the inverse contrast (Successful Go>Successful Stop) in the same regions to ascertain that any observed between-group differences in brain activation were specific for inhibition and not related to Go-trial processing. Error-related activity (Failed Stop>Successful Stop) was examined in the anterior cingulate cortex, using a spherical ROI around the coordinates [x=-3, y=20, z=34].

Analyses on group interaction effects were conducted with and without mean SSRT as a nuisance covariate (interacting with group) to correct for inter-individual differences in task-performance and masked by the group-specific main effects of task (inclusive, P<.05). Results were considered significant if they fell below an alpha of P<.017, FWE-corrected. This critical value was established with SISA (http://www.quantitativeskills.com/sisa/calculations/bonhlp.htm), which uses the mean correlation between variables (r= 0.43) that are mutually correlated (i.e. activity in seven ROIs) for the alpha correction and allows one to perform a less stringent correction than the Bonferroni method for multiple comparisons. Between-group differences with a significance between .017<P<.05, FWE-corrected are also reported. Furthermore, we explored these effects with a whole-brain analyses at a more lenient threshold of P<.001, uncorrected (see figure S6.1 and Table S6.1).

In order to establish the behavioral and clinical relevance of the between-group differences in task-related BOLD response, we correlated within-group BOLD activity with behavioral measures, UPDRS-III and dopamine transporter (DaT) availability using a ROI approach. Spherical ROIs with a radius of 20 mm were constructed around the peak voxel of clusters that showed between-group

differences at P<.05, FWE corrected (see Table 6.2) and masked each spherical ROI with the cluster specific Brodmann area (2x dilated, WFU Pickatlas, Wake Forest University, Winston-Salem, NC, USA) to increase specificity. For example, for the right IFG a 20 mm spherical ROI was constructed around MNI coordinates x=51, y=20, z=4 (see Table 6.2) and masked with voxels within Brodmann area 47. Mean BOLD activity was extracted per subject from these ROIs using MarsBaR (http://marsbar.sourceforge.net/) and correlations with clinical and behavioral measures were performed in SPSS. Mean activity in these ROIs was also correlated with DaT availability in the posterior putamen, anterior-dorsal striatum and ventral striatum, conform (Vriend *et al.* 2014b). For behavioral and clinical analyses in SPSS alpha was set to P<.05; we considered P<.1 a trend.

Results

Demographic and behavioral analyses – group differences

Parkinson patients (N=21) and healthy controls (N=37) were matched for age, gender and intelligence (Table 1). There were also no differences in MMSE score and none of the participants showed signs of dementia (MMSE ≤24). Measures of disease stage, disease duration and severity of motor symptoms are presented in Table 6.1. Go-trial reaction times were longer in Parkinson patients compared with healthy controls (t(56)= 2.50, P=.02). SSRT was also slightly longer in Parkinson patients (259.5±62.5) compared with healthy controls (238.8±41.8) although this difference failed to reach significance (t(56)= 1.50, P=.14). Parkinson patients made fewer erroneous responses to Stop-trials than healthy controls (U=244, P=.02), but there were no between-group differences in the Go-trial error percentage (see Table 6.1).

Behavioral analyses – correlations

Age did not correlate with SSRT in either group, but did correlate positively with Go-trial reaction time in healthy controls but not Parkinson's disease (healthy controls: r=0.42, P=.009; Parkinson's disease: r=0.29, P=.20). Severity of motor symptoms in Parkinson patients, as measured by the UPDRS-III, correlated positively with Go-trial reaction time (r=0.50, P=.02) but not SSRT (r=0.35, P=.12), which exemplifies that SSRT slowing is unrelated to Parkinson-related motor impairments.

Imaging analyses – task effects across and within groups

During inhibition (successful Stop>successful Go) task-related brain activation was observed in the inferior frontal gyrus, pre-supplementary motor area extending into the dorsolateral prefrontal cortex, caudate nucleus, inferior parietal cortex and precuneus (see figure S6.1). Task-related brain activation was largely right lateralized in Parkinson's disease, while in healthy controls more

bilateral activity was observed. The error-related contrast (failed Stop>successful Stop) showed involvement of the dorsal anterior cingulate cortex, bilateral precentral gyri and occipital cortex.

Imaging analyses – task effects across and within groups

During inhibition (successful Stop>successful Go) task-related brain activation was observed in the inferior frontal gyrus, pre-supplementary motor area extending into the dorsolateral prefrontal cortex, caudate nucleus, inferior parietal cortex and precuneus (see figure S6.1). Task-related brain activation was largely right lateralized in Parkinson's disease, while in healthy controls more bilateral activity was observed. The error-related contrast (failed Stop>successful Stop) showed involvement of the dorsal anterior cingulate cortex, bilateral precentral gyri and occipital cortex.

Imaging analyses – between-group differences

During successful inhibition, Parkinson patients compared with healthy controls, showed significantly decreased activity in the right (x=51, y=20, z=4, ke=16, PFWE=.015) and left (x=-57, y=11, z=7, ke=6,PFWE=.011) inferior frontal gyrus (see Figure 5. 1a,b and Table 5.2). Task-related activity in the inferior parietal lobule (x=-33, y=-61, z=34, ke=3, PFWE=.042) was also decreased in Parkinson patients but fell short of the alpha-level determined by SISA (PFWE<.017). Parkinson patients showed no task-related activity increases compared with healthy controls and there were no differences in error-related or Go-trial processing. Including SSRT as a nuisance covariate had no effect on the reported results. The exploratory whole-brain analyses showed additional decreases in activity in the bilateral cerebellum, right precuneus, right caudate nucleus and right occipital temporal area during successful inhibition and a cluster of decreased activity in the right posterior cingulate cortex during error-processing (Table S6.1 and Figure S6.2).

Imaging analyses – Correlations with clinical and behavioral measures

In Parkinson's disease, UPDRS-III correlated negatively with inhibition-related activity in the left IFG (r=-.53,P=.01; see figure 6.2). There were no significant correlations between task performance and inhibition or error-related activity in Parkinson's disease. In healthy controls, Go-trial reaction times correlated negatively with inhibition-related activity in the right IFG (r= -.33, P=.04).

For fifteen Parkinson patients [123I]FP-CIT SPECT imaging data were available. The interval between SPECT and fMRI imaging was on average 56(±28) days. DaT availability did not correlate with task performance, UPDRS-III or error-related activity. DaT availability in the left and right ventral striatum, but not anterior-dorsal striatum and posterior putamen, correlated positively with inhibition-related activity (successful Stop>Successful Go) in the right IFG (left: r=.69, P=.004, right: r=.66, P=.007, figure S6.3). Nevertheless, when adding age as a control

Table 6.1 – Demographics, clinical measures and task performance

	Parkinson	healthy controls	Test statistic (P-value)
N patients (% male)	21 (71.4)	37 (56.8)	1.22 (.27)a
Age	59.0 ± 10.4	56.2 ± 9.9	1.01 (.32)b
IQ estimation	104.0 ± 18.9	104.5 ± 13.8	-0.11 (.91)b
Handedness (L/R)	3/18	4/33	.15 (.70)a
MMSE	28.8 ± 0.9	29.1 ± 0.8	312.5 (.19)c
UPDRS III	21.6 ± 8.3		
H&Y stage	1.9 ± 0.4		
Disease duration (weeks)	10.5 ± 16.3		
Go-trial reaction time (ms)	780.1 ± 126.3	688.4 ± 138.2	2.50 (.02)b
SSRT (ms)	259.5 ± 62.5	238.8 ± 41.8	1.5 (.14)b
Go-trial error (%)	3.2 ± 5.4	1.5 ± 1.8	337.5 (.40)c
Stop-trial error (%)	41.7 ± 4.2	44.8 ± 4.4	244 (.02) c

a= chi-square test, b= two-sample T-test, c= Mann-Whitney U-test. Abbreviations: MMSE = Mini Mental State Examination, UPDRS III = Unified Parkinson's disease rating scale part III (motor section), H&Y= Hoehn & Yahr, SSRT = stop signal reaction time.

variable to the correlation these associations were no longer significant (left: r=.42, P=.14, right: r=.31, P=.28). Age correlated negatively with DaT availability in the left (r=-.75, P=.001) and right ventral striatum (r=-.81, P<.001) and right IFG activation (r=-.64,P=.01). These negative correlations with age are consistent with previous studies (Sebastian *et al.* 2013a; Varrone *et al.* 2013; Vriend *et al.* 2014d). The presented correlation between DaT availability and IFG activation 'corrected' for age may, however, have been biased, especially in this relatively small sample and should be considered with caution. When two independent variables are highly correlated, partial correlations with a dependent variable become unstable and prone to sampling errors (i.e. problem of multi-collinearity) (Blalock 1963; Cramer 2003).

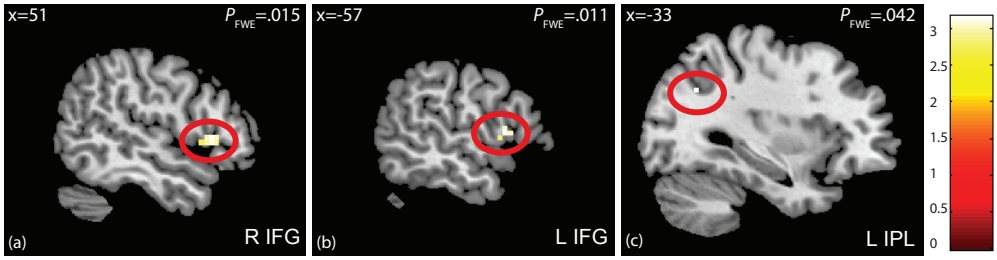

Figure 6.1 – Group x task effects during inhibition in Parkinson's disease (N=21) and matched healthy controls (N=37). Hypoactivated voxels during inhibition (contrast: successful Stop>successful Go) in the right inferior frontal gyrus (a), left inferior frontal gyrus (b) and left inferior parietal lobule (c) in Parkinson's disease patients compared with healthy controls. See Table 2 for coordinates and statistics.

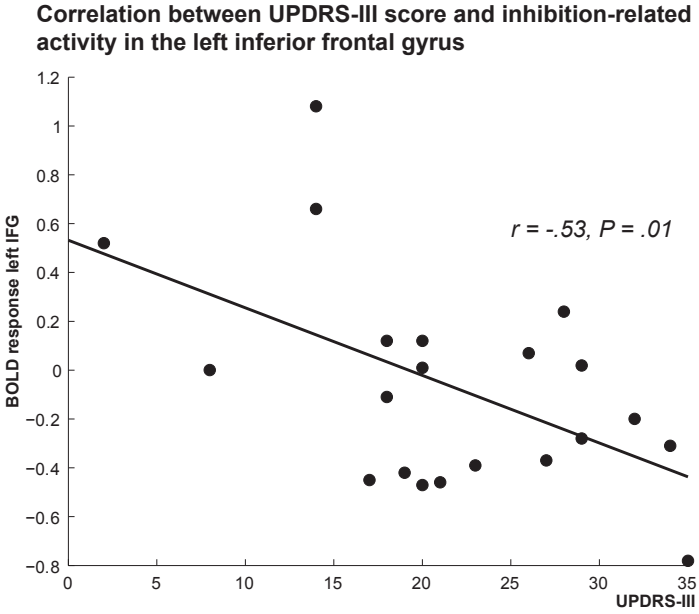

Figure 6.2 – Correlation between UPDRS-III and inhibition-related activity in the left inferior frontal gyrus. Abbreviations: IFG = inferior frontal gyrus, UPDRS-III = Unified Parkinson's Disease Related Symptoms Rating Scale part III (motor section). BOLD = Blood oxygen level dependent.

Table 6.2 – Group x task effects during inhibition and error processing

							MNI coordinates		
Contrast	**Anatomical region**	**BA**	**L/R**	**ke**	**t**	**P_{FWE}**	**x**	**y**	**z**
INHIBITION									
PD>HC	no significant findings								
PD<HC	**inferior frontal gyrus**	**44**	**L**	**6**	**3.53**	**.011**	**-57**	**11**	**7**
		47	**R**	**16**	**3.57**	**.015**	**51**	**20**	**4**
	Inferior parietal lobule	39	L	3	3.17	.042	-33	-61	34
ERROR									
PD>HC	no significant findings								
PD<HC	no significant findings								

Anatomical regions printed in bold are significant at P<.017, the critical value determined by SISA to correct for multiple comparisons. Abbreviations: PD = Parkinson's disease, HC=healthy controls, BA = Brodmann Area, Ke= cluster size

Discussion

A growing body of literature indicates impaired response inhibition in Parkinson patients. The novelty of this study lies in the fact that all Parkinson patients were naïve for dopamine replacement therapy, which excludes the possible confounding effects of (chronic) medication use on behavioral performance and functional activity during a response inhibition task. Compared with matched healthy controls, Parkinson patients showed hypoactivation of inhibition-related brain areas such as the IFG and inferior parietal lobule during execution of a stop-signal task. In contrast, previous neuroimaging studies employing the Go/No-Go task in Parkinson patients versus healthy controls showed mainly hyperactivated brain regions and no differences in task performance (Farid *et al.* 2009; Baglio *et al.* 2011). The disparity with our results is most likely explained by the fact that the Go/No-Go task exerts lower inhibitory demands than the stop-signal task (Aron 2011; Sebastian *et al.* 2013a). In the Go/No-Go task, Parkinson patients have the opportunity to boost their performance by recruiting additional inhibition-related brain areas; e.g. contralateral brain areas and the cerebellum. If inhibitory demands are higher, such as in the stop-signal task, these compensation mechanisms fail and performance declines. This is consistent with the so-called 'compensation-related utilization of neural circuits hypothesis' (CRUNCH) of normal aging (Reuter-Lorenz and Lustig 2005). Bearing this hypothesis in mind, the hypoactivation of inhibition-related brain areas in Parkinson's disease versus healthy controls may be seen as accelerated aging in Parkinson patients (Collier *et al.* 2011). This between-group difference in the capacity to compensate can be

visualized by a shift in the inverse U-shaped relation between task demands and inhibition-related neural circuit activity during response inhibition that we recently proposed (van Velzen *et al.* 2014). The cause of this shift remains speculative although we suggested that dysfunction of striatal dopamine signaling might be a prime suspect due to its major neuromodulatory role in the cortico-striatal-thalamocortical circuits that subserve goal-directed behavior (Alexander *et al.* 1986). Nevertheless, there is ample evidence that other neurotransmitters such as serotonin and noradrenalin also play a role in response inhibition (see Dalley and Roiser 2012; Bari and Robbins 2013a for reviews) and further research is therefore warranted. Our negative correlation between left IFG activity and UPDRS-III score is consistent with a further shift in the relation between task demands and inhibition-related neural circuit activity as disease severity progresses.

Our results are also consistent with recent results (Ye *et al.* 2014b) describing a decreased activation of the right inferior frontal gyrus in medicated Parkinson's disease patients compared with healthy controls. Unlike Ye *et al.* and contrary to our expectations, we did not observe a significantly increased SSRT in Parkinson patients. This is also in contrast with other studies employing the stop-signal task in Parkinson's disease versus healthy controls (Gauggel *et al.* 2004; Obeso *et al.* 2011a; Obeso *et al.* 2011b). Nevertheless, these studies employed the mean method to estimate SSRT (mean Go-RT - mean SSD) that has recently been shown to consistently overestimate the SSRT (Verbruggen *et al.* 2013). It is therefore possible that some of the reported differences might actually have been overestimated. When using the mean method Parkinson patients had a significantly slower SSRT than healthy controls (Parkinson 269.1±49.4; healthy control: 243.8±44.4; $t(56)= 2.0$, $P=.049$). Another explanation might be that our task was optimized for use during fMRI scanning and consisted of fewer trials than other studies employing the stop-signal task in Parkinson's disease (Gauggel *et al.* 2004; Obeso *et al.* 2011a; Obeso *et al.* 2011b; Ye *et al.* 2014b) and might thus have been underpowered to capture subtle between-group behavioral differences. A last possible explanation might be that our early stage medication-naïve Parkinson patients -- although they showed clear functional impairments -- were still relatively behaviorally preserved. Since this is the first study to investigate response inhibition in de novo Parkinson's disease we are unable to ascertain which explanation is correct. Whether or not de novo Parkinson patients already show behavioral deficits in response inhibition therefore warrants further investigation.

Impairments in response inhibition reflect deficits in impulse control that can grow into impulse control disorders (ICD). These disorders develop in at least 14% of all Parkinson's disease patients that receivedopamine replacement therapy (Weintraub *et al.* 2010a; Vriend *et al.* 2014c). Examples of ICD include pathological gambling, hypersexuality, compulsive shopping and compulsive eating (Weintraub *et al.* 2010a; Vriend *et al.* 2014c) and the development is thought to depend on an interaction between a pre-morbid neurobiological susceptibility and the use of dopamine replacement therapy. The exact nature

of this neurobiological susceptibility is still under investigation, although we previously showed that the development of ICD symptoms is predated by a more pronounced striatal dopaminergic denervation, as measured by dopamine transporter availability, compared with patients not developing ICD symptoms (Vriend *et al.* 2014b). Based on this study and others (Cilia *et al.* 2010; Lee *et al.* 2013; Voon *et al.* 2014) we hypothesize that the development of ICD is partly governed by dopaminergic denervation due to the Parkinson's disease pathology and concomitant dysfunction of cortico-striatal-thalamocortical circuits (see Vriend *et al.* 2014c for review). In this regard, the correlation between ventral striatal DaT availability and inhibition-related activity in the right inferior frontal gyrus is of interest and indicates that higherdopamine denervation of the ventral striatum was associated with less inhibition-related activity. This suggests a direct role of the Parkinson pathology in impulse control deficits. The correlation between striatal dopamine transporter availability and task-related activation of the right inferior frontal gyrus did, however, not survive adjustment for age, probably due to a lack of power, and further investigation in a larger study sample is therefore warranted.

In this study we chose to examine impulse control deficits in de novo Parkinson's disease patients without neuropsychiatric symptoms, despite the fact that clinically significant deficits in impulse control (i.e. ICD) almost exclusively develop in Parkinson's disease after the start of dopamine replacement therapy (Weintraub *et al.* 2010a; Vriend *et al.* 2014c). Nevertheless, previous studies have shown that deficits in impulse control and reward processing are also evident in Parkinson's disease patients without ICD (Aarts *et al.* 2012; van der Vegt *et al.* 2013; Ye *et al.* 2014b) and our design allowed us to specifically examine the effects of the Parkinson pathology on impulse control deficits which are not obscured by (chronic) medication effects or neuronal alterations associated with the development of ICD. It is currently unknown whether pre-morbid decreased inhibition-related brain activity constitutes an increased risk of later developing ICD, although clinical evidence suggests that a (family) history of impulsivity increases the risk of developing ICD (Weintraub *et al.* 2010a).

A possible limitation of this study is that we employed a stop-signal task paradigm that contained fewer trials than other previous response inhibition tasks used in Parkinson's disease which may have hampered our ability to correctly estimate the SSRT and underpowered our behavioral analysis. Further studies are therefore needed to investigate whether de novo Parkinson's disease patients already show impairments at the behavioral level.

In conclusion, this study is the first to study the neural correlates of the stop-signal task in de novo Parkinson patients. We showed that, compared with well-matched healthy controls, Parkinson patients exhibit functional impairments in motor inhibition that are partly related to disease severity. This study provides insights into the neural underpinnings of impulse control deficits in PD and provides possible leads for the investigation of the neurobiological susceptibility

that may lead to the development of medication-induced ICD in Parkinson's disease.

Supplementary Methods

Stop-signal task

The stop-signal task utilized in this study was previously described by (de Wit *et al.* 2012). The task consisted of 252 trials, of which 80 percent were Go-trials where participants had to indicate the orientation of an arrow (left or right) with a button-press by the accordant index finger. The number of stimuli pointing to the left and right were equal to limit the (dis)advantage that left or right handers might experience during the task. The remaining 20% of the trials were Stop trials. Stop trials began similar to Go-trials. In both cases a fixation cross was presented for 500 ms after which an arrow appeared for a maximum of 1000 ms. In stop-trials a cross was additionally superimposed on the arrow after a variable delay after the appearance of the arrow (stop-signal delay or SSD). The SSD was continuously adapted by a staircase tracking mechanism. At the beginning of the task the SSD was set to 250 ms and updated according to the performance of the participant. The SSD of the following Stop trial was decreased by 50 ms after a failed stop-response (i.e. a response was given) and increased by 50 ms after a successful stop-response (i.e. no response was given) to approximate a 50 percent inhibition on all stop trials. Go and Stop trials were pseudo-randomly intermixed with the first 12 trials being Go-trials and that Stop-trials never succeeded each other. The intertrial interval jittered randomly between 1500 and 2500 ms. Participants performed a practice run prior to MRI scanning to familiarize them with the task and they were instructed to respond as quickly and accurately as possible. They were also told that the design of the task would prevent them from accurately inhibiting their responses on all Stop-trials.

Task presentation and behavioral recordings were performed with E-Prime 1.2 (Psychology Software Tools, Pittsburgh, PA, USA). Stimuli were presented on a screen behind the participant's head at the end of the scanner table, which was visible through a mirror mounted on the head coil. Responses were given with an MRI-compatible response box (Current Designs, Philadelphia, PA, USA).

Dopamine transporter (DaT) SPECT imaging - procedure

We used the established [123I]FP-CIT ([123I]N-ω-Fluoropropyl-2β-carbomethoxy-3β-(4-iodophenyl)nortropane) SPECT tracer to measure presynaptic striatal dopamine transporter availability, an often utilized marker for the integrity of dopaminergic projections towards the striatum (Scherfler *et al.* 2007) . All patients received oral potassium perchlorate to block thyroid uptake of free radioactive iodide. [123I]FP-CIT was injected intravenously three hours before image acquisition at an approximate dose of 185 MBq (specific activity >185

MBq/nmol; radiochemical purity >99%). Subjects were imaged using a dual-head gamma camera (E.Cam; Siemens, Munich, Germany) with a fan-beam collimator. We acquired 60 x 30 second views per head over a 180° orbit on a 128×128-pixel matrix resulting in a total imaging time of 30 minutes. Image reconstruction was performed using a filtered back projection with a Butterworth filter (order 8, cutoff 0.6 cycles/cm; voxel size: 3.9 mm3 after reconstruction). Scans were reoriented manually to ensure that left and right striatum were aligned.

DaT SPECT imaging – image processing

Preprocessing steps and analyses of the DaT SPECT scans were performed in SPM8 (Wellcome Trust Center for Neuroimaging, London, UK). Scans were co-registered to each individual's structural T1 image. T1 images were normalized to Montreal Neurological Institute (MNI) space and we applied the resulting normalization parameters to the co-registered DaT SPECT scan. DaT SPECT scans were subsequently resliced to a voxel size of 2mm3 using trilinear interpolation and spatially smoothed with a 6 mm FWHM Gaussian kernel to correct for inter-individual anatomical differences.

Binding ratios and regions of interest

Individual binding ratios (BR) of specific to non-specific DaT binding were calculated for the left and right ventral striatum, anterior-dorsal striatum (aDS) and posterior putamen (PP), cf. (Vriend *et al.* 2014b). Tracer binding in the bilateral superior, medial and inferior occipital gyri was used as a reference. The VS was defined according to the method described by Tziortzi *et al.* (2011) (Tziortzi *et al.* 2011) and traced on the coronal slices of a standard single subject T1-weighted MRI scan available in SPM8. The aDS was delineated on the same coronal slices as the VS. To avoid spillover effects, a gap of approximately 5 mm was left between the borders of the VS and aDS. These voxels were excluded from BR calculation. We based the PP ROI on the putamen ROI from the AAL (Automated Anatomical Labeling) atlas such that it comprised only voxels posterior to the anterior commissure (Helmich *et al.* 2010; Aarts *et al.* 2012). Mean DaT availability was extracted from these ROIs using MarsBaR (http://marsbar.sourceforge.net/) and Pearson's (semi-partial) correlations were performed in SPSS. Results were considered significant if they fell below an alpha of P<.018. This critical value was established with SISA (http://www.quantitativeskills.com/sisa/calculations/bonhlp.htm), which uses the mean correlation between variables (r= 0.44) that are mutually correlated (i.e. DaT binding in six ROIs) for the alpha correction to allow for a less stringent correction than the Bonferroni method for multiple comparisons.

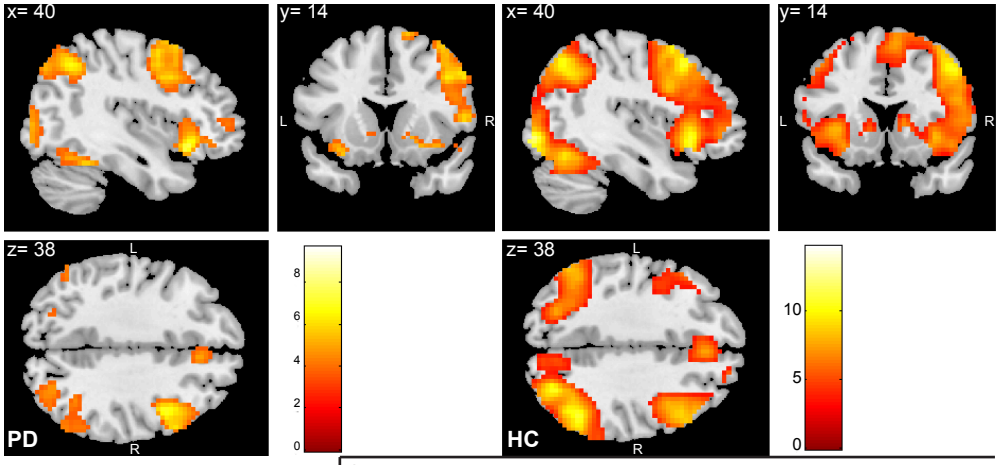

Figure S6.1 (above) – Main effect of inhibition-related activity in Parkinson's disease patients (N=21) and matched healthy controls (N=37). Activity is presented at P<.001, uncorrected.

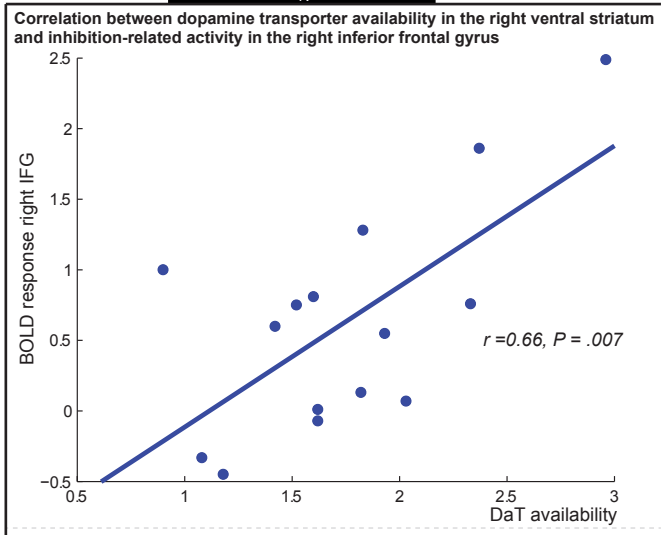

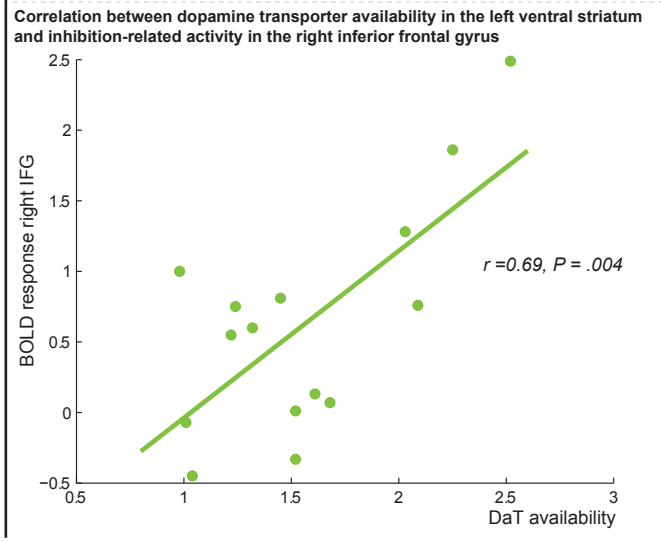

Figure S6.3 (right) – Correlation between ventral striatal dopamine transporter availability and inhibition-related activity in the right inferior frontal gyrus.

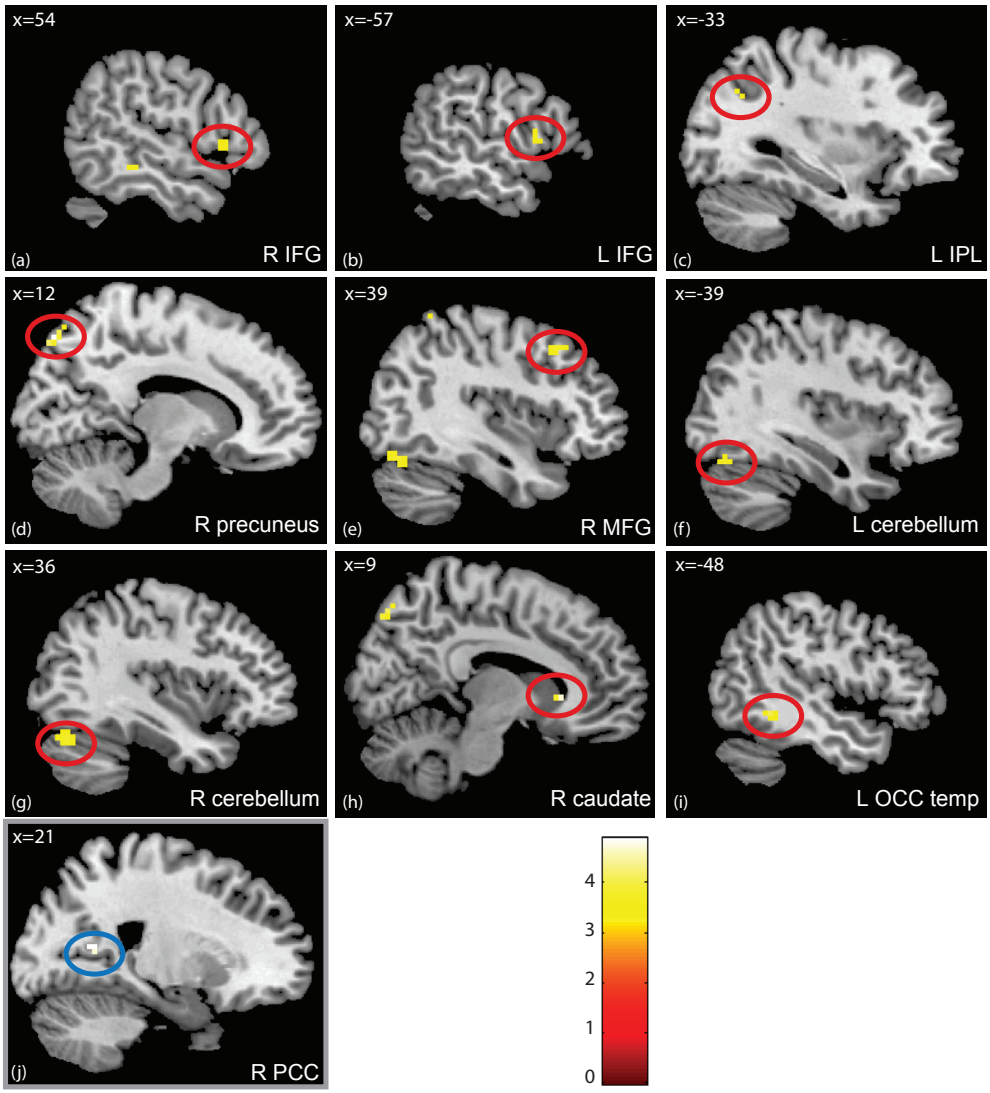

Figure S6.2 – Group x task effects during inhibition and error processing in Parkinson's disease patients (N=21) and matched healthy controls (N=37). (a-i) hypoactivated voxels in Parkinson's disease patients compared with healthy controls during inhibition (contrast: successful Stop>successful Go). (j) hypoactivated voxels in Parkinson's disease patients compared with healthy controls during error processing (contrast: failed Stop>successful Stop). Results presented at P<.001, uncorrected. See supplementary Table 1 for coordinates and statistics.

Table S6.1 – Group x task effects of inhibition and error-related activity (P<.001, uncorrected)

				MNI coordinates				
Contrast	Anatomical region	BA	L/R	ke	t	x	y	z
INHIBITION								
PD>HC	no significant findings							
PD<HC	Occipito-temporal area	37	L	27	4.65	-48	-46	-8
	Precuneus	7	R	18	4.50	12	-79	52
	Caudate nucleus		R	4	4.44	9	23	1
	inferior frontal gyrus	44	L	8	4.05	-57	8	10
		47	R	7	3.47	51	20	4
	Cerebellum		R	26	4.03	36	-73	-20
			L	23	3.76	-42	-70	-23
	Middle frontal gyrus	8	R	7	3.61	39	20	46
	Inferior parietal lobule	39	L	3	3.26	-33	-64	37
ERROR								
PD>HC	no significant findings							
PD<HC	Posterior cingulate	30	R	8	3.50	21	-55	13

Abbreviations: PD = Parkinson's disease, HC=healthy controls, BA = Brodmann area, Ke= cluster size